Circulation: Cardiovascular Imaging

ORIGINAL ARTICLE

Echocardiographic Characterization of Myocardial Stiffness in Healthy Volunteers, Cardiac Amyloidosis, and Hypertrophic Cardiomyopathy: A Case-Control Study Using Multimodality Imaging

Dominik C. Benz, MD; Ali Sadeghi, PhD; Pat G. Rafter, MS; Olivier F. Clerc, MD, MPH; Jocelyn Canseco Neri, MS; Alexandra Taylor, BS; Shilpa Vijayakumar, MD, MPH; Carolyn Y. Ho, MD; Sarah A.M. Cuddy, MD; Rodney H. Falk, MD; Sharmila Dorbala, MD, MPH

BACKGROUND: Noninvasive tools to measure myocardial stiffness are limited. Intrinsic cardiac elastography in echocardiography relates to myocardial stiffness by measuring the propagation of the myocardial stretch generated by atrial contraction. The aims of the present study were (1) to evaluate myocardial stiffness using intrinsic cardiac elastography in healthy volunteers versus those with myocardial diseases (ie, cardiac amyloidosis [CA] and hypertrophic cardiomyopathy) and (2) to identify key factors that affect myocardial stiffness.

METHODS: In this prospective study, myocardial stiffness was estimated in 54 participants, including 10 hypertrophic cardiomyopathy, 28 CA, and 16 healthy volunteers. Myocardial stiffness was assessed as intrinsic velocity propagation of myocardial stretch (iVP, m/s) measured by high frame rate echocardiography (ie, above 250 frames per second). Extracellular volume was quantified by cardiac magnetic resonance in 22 participants. Amyloid burden was quantified by cardiac amyloid activity in ^{99m}Tc-labeled pyrophosphate single-photon emission computed tomography in 10 participants.

RESULTS: Myocardial stiffness was significantly higher in the CA cohort (median iVP, 2.6 m/s; interquartile range, 1.7–3.9 m/s) than in the hypertrophic cardiomyopathy cohort (median iVP, 1.4 m/s; interquartile range, 1.0–1.8 m/s; P=0.011). In patients with CA or hypertrophic cardiomyopathy, iVP was correlated with NT-proBNP (N-terminal pro-B-type natriuretic peptide) (ρ=0.498, P=0.003), extracellular volume (ρ=0.646, P=0.004), and cardiac amyloid activity (ρ=0.891, P<0.001). In multivariate linear regression analysis, extracellular volume was independently associated with myocardial stiffness even after accounting for indexed left ventricular mass, global longitudinal strain, and E/e'. In healthy volunteers, normal myocardial stiffness was defined by the upper limit of normal of iVP at 1.7 m/s. Patients with CA and normal myocardial stiffness (iVP <1.7 m/s) were characterized by a low risk profile including lower NT-proBNP (P=0.034), lower troponin T (P=0.041), lower National Amyloidosis Center stage (P=0.031), smaller interstitial expansion (P=0.014), and smaller amyloid burden (P=0.056).

CONCLUSIONS: Intrinsic cardiac elastography is a reliable noninvasive tool to measure myocardial stiffness. In this pilot study, it is related to imaging markers of interstitial expansion and amyloid burden.

GRAPHICAL ABSTRACT: A graphical abstract is available for this article.

Key Words: amyloidosis ■ cardiomyopathies ■ cardiomyopathy, hypertrophic ■ echocardiography ■ elasticity imaging techniques

See Editorial by Espeland and Aakhus

Correspondence to: Sharmila Dorbala, MD, MPH, Cardiac Amyloidosis Program, Division of Cardiology, Department of Medicine, Cardiovascular Imaging Program, Division of Nuclear Medicine and Molecular Imaging, Department of Radiology, Brigham and Women's Hospital and Harvard Medical School, 75 Francis St, Boston, MA 02115. Email sdorbala@bwh.harvard.edu

Supplemental Material is available at https://www.ahajournals.org/doi/suppl/10.1161/CIRCIMAGING.124.017475.
For Sources of Funding and Disclosures, see page XXX.

Circulation: Cardiovascular Imaging is available at www.ahajournals.org/journal/circimaging

CLINICAL PERSPECTIVE

Myocardial stiffness is associated with risk of heart failure, but noninvasive assessment of myocardial stiffness remains challenging. This study demonstrates and confirms the feasibility and clinical value of intrinsic cardiac elastography, a novel noninvasive tool to quantify myocardial stiffness. Using high frame rate echocardiography, this technique quantifies myocardial stiffness by visualizing myocardial mechanical waves induced by atrial contraction. Our findings reveal higher myocardial stiffness in cardiac amyloidosis, compared to healthy volunteers and to participants with hypertrophic cardiomyopathy. Myocardial stiffness correlated closely with extracellular volume on magnetic resonance imaging and to quantitative cardiac amyloid burden estimated by Tc-99m-pyrophosphate single-photon emission computed tomography. Notably, participants with normal myocardial stiffness (<1.7 m/s) had a lower risk profile, including lower cardiac biomarker levels, lower amyloid burden measures, and lower risk prognostic staging. Our pilot study suggests that myocardial stiffness by intrinsic cardiac elastography may unveil a novel window into heart failure disease biology. Future prospective studies should address the value of myocardial stiffness to guide heart failure management on top of N-terminal pro-B-type natriuretic peptide.

Nonstandard Abbreviations and Acronyms

AL	light chain
ATTR	transthyretin
CA	cardiac amyloidosis
CMR	cardiac magnetic resonance
CT	computed tomography
ECV	extracellular volume
EF	ejection fraction
GLS	global longitudinal strain
HCM	hypertrophic cardiomyopathy
iVP	intrinsic velocity propagation
LA	left atrial
LV	left ventricle
LVMi	indexed left ventricular mass
PYP	pyrophosphate
RV	right ventricle
SPECT	single-photon emission computed tomography

Myocardial stiffness remains a key determinant of heart failure. Currently, the reference standard for myocardial stiffness is invasive pressure-volume loop indices, and noninvasive tools to measure myocardial stiffness are limited. Conventional echocardiographic parameters (ie, pulse-wave and tissue Doppler imaging) classify diastolic function based on complex algorithms and derive surrogate information on myocardial properties that may be ambiguous. However, recent technological refinements allow myocardial stiffness to be quantified directly by intrinsic cardiac elastography.[1] The framework is based on detecting myocardial mechanical waves that are induced by intrinsic cardiac events and propagate throughout the myocardium at velocities from 1 to 10 m/s, with stiffer myocardium resulting in faster mechanical waves.[2] Atrial contractions are hypothesized to generate a pressure wave from the blood vortex that propagates from the base to the apex.[3] Its relation to myocardial stiffness is based on the theory of waves traveling in elastic tubes (the Moens-Korteweg equation).[4] Currently, conventional B-mode imaging in clinical echocardiography is limited to a temporal resolution of 50 to 100 frames per second (fps) and cannot resolve short-lived myocardial mechanical waves. By using broad transmission beams from diverging wave sequences, high frame rate echocardiography can achieve high temporal resolution and detect myocardial mechanical waves.[2] Previously, increased myocardial stiffness was demonstrated in cardiac amyloidosis (CA) by intrinsic cardiac elastography based on tissue Doppler imaging.[5] In the present study, we applied a new approach using coherent compounding of the diverging beams to detect myocardial mechanical waves.

The aims of this study were as follows: (1) to assess the clinical value of intrinsic cardiac elastography in characterizing myocardial stiffness in healthy volunteers and myocardial diseases (ie, CA and hypertrophic cardiomyopathy [HCM]) and (2) to identify the key factors among clinical characteristics, serological biomarkers, and markers from echocardiography, cardiac magnetic resonance (CMR), and bone avid tracer cardiac scintigraphy that affect myocardial stiffness estimated by intrinsic cardiac elastography.

METHODS

The data that support the findings of this study are available from the corresponding author upon reasonable request.

Study Population

The study was approved by the Mass General Brigham Human Research Committee, and each participant provided written informed consent. This cross-sectional clinical study recruited 63 participants between February and December 2022, including healthy volunteers (n=17) as well as patients with HCM (n=11), ATTR (transthyretin) CA (n=26), and light chain (AL) CA (n=9). Patients were recruited at Brigham and Women's Hospital, Boston, MA, at the time of echocardiography. Healthy volunteers were recruited as controls to establish normal limits and test repeatability and were examined at Philips Research North America (Cambridge, MA). Of the enrolled 63 participants,

measurement of intrinsic velocity propagation (iVP) was feasible in 52 participants (83%); it failed in 9 participants (5 with cardiac ATTR amyloidosis, 2 with cardiac AL amyloidosis, 1 with HCM, and 1 healthy control) due to unexpected atrial fibrillation, intermittent RV pacing, or other factors (eg, fusion of E and A wave).

HCM was diagnosed as unexplained left ventricular (LV) hypertrophy in the absence of other cardiac and systemic disease and with maximal LV thickness of at least 15 mm, and the study included only HCM patients with typical asymmetrical septal hypertrophy. AL CA was diagnosed using standard criteria for systemic AL amyloidosis, including biopsy with confirmation of amyloid type by immunohistochemistry or mass spectrometry and proof of cardiac involvement by imaging or endomyocardial biopsy.[6] ATTR CA was diagnosed by a grade 2/3 cardiac 99mTc-pyrophosphate (PYP) single-photon emission computed tomography (SPECT)/computed tomography (CT) scan and exclusion of AL amyloidosis by serum free light chain assay and serum and urine immunofixation electrophoresis, or by endomyocardial biopsy with immunohistochemistry or mass spectrometry.[6]

Exclusion criteria were known persistent atrial fibrillation and permanent right ventricular (RV) pacing.

Standard Echocardiography

All patients (excluding healthy volunteers) underwent comprehensive transthoracic imaging as clinically indicated, and measurements were performed according to current recommendations using dedicated software (Tomtec Image Arena, version 4.6; Tomtec Imaging Systems GmbH, Unterschleissheim, Germany).[7] LV, left atrial (LA), and RV myocardial strain were quantified by speckle-tracking from B-mode data acquired in 3 standard apical views (4-chamber, 2-chamber, and long-axis views) using dedicated software (Tomtec Image Arena). Frame rates were between 50 and 70 fps. LV global longitudinal peak strain (GLS) was obtained by averaging 18 segmental values from the apical views.

Intrinsic Cardiac Elastography

Acquisition

All participants (including healthy volunteers) underwent high frame rate echocardiography (>250 fps; median, 252 fps [interquartile range (IQR), 252–254 fps]) on an Epiq CVx ultrasound machine with a clinical X5-1 transducer (Philips Healthcare, Cambridge, MA) using coherent compounding of broad transmission beams from diverging wave sequences. Since transmits are diverging but remain relatively narrow, few transmits were coherently combined to minimize motion artifacts. A negative transmit focus (behind the probe) was chosen to maximize beam overlap and improve the coherent compounding. The sector width and image depth were minimized to focus the apical field of view on the interventricular septum. Images were acquired over 3 cardiac cycles.

Repeatability Measurements

Image acquisition was repeated 3× for each participant to assess repeatability.

Signal Processing

The operator performing signal processing and velocity measurement was blinded to the clinical data, including disease pathology. First, the myocardial midline in the region of interest (along the inferoseptum) was manually traced on the first log-detected, scan-converted frame of the sequence. Subsequently, this midline was rigidly translated and rotated to track the motion of the region of interest using the Demons algorithm and a large smoothing kernel size.[8] Second, a high-pass clutter suppression filter was applied to radiofrequency data across frames in the slow time dimension to remove stationary clutter echoes from reverberations in the chest wall (Figure S1).[9] A cutoff tissue velocity of 1 cm/s was used for the clutter filter. Third, radial tissue motion (within the region of interest) was tracked twice with standard 1-dimensional cross-correlation along the beam: once with and once without preprocessing with the clutter filter. The 2 resulting velocity maps were merged by keeping for each pixel the velocity with the preprocessing (clutter filtering or not) that locally yielded the highest cross-correlation coefficient.[10] Fourth, the computed radial velocities along the inferoseptum were displayed as a curved anatomic M-mode (horizontal axis: time; vertical axis: distance along the septum).

Velocity measurement

The mechanical wave induced by atrial contraction and propagating from base to apex during late diastole was illustrated as an isovelocity wave front (ie, intrinsic velocity propagation of myocardial stretch, or iVP [in m/s]). In our experience, the signal was least affected by cardiac motion and reverberation artifacts, and the angle error was smallest at the inferoseptal wall. Prior studies have confirmed that iVP from atrial contraction at the inferoseptum can be acquired most consistently.[3] A semi-automatic random sample consensus algorithm was used to measure the intrinsic velocity propagation of the mechanical wave along the inferoseptum. Random sample consensus is a widely used, iterative linear fitting method to interpret data with a significant number of outliers.[11] The upper limit of normal iVP was defined as the 95th percentile in healthy volunteers.

Cardiac Magnetic Resonance

Clinically indicated CMR studies were performed with native and postcontrast T1 mapping for quantification of myocardial extracellular volume (ECV) using the modified look-locker technique (with a 5-3-3 pattern) was performed on a 3.0-T system (Tim Trio; Siemens). Segmental ECVs were calculated by the ratio of changes of relaxation rates of the myocardium to relaxation rates of blood and adjusted to the fractional blood volume of distribution (1 − hematocrit). Inferoseptal myocardial ECV was then calculated by a single observer averaging the myocardial segmental ECVs from the short-axis slices at the base, mid, and apical LV levels. A commercial software package (MedisSuite, version 3.0; Medical Imaging Systems) was used to process and quantify the ECVs.[12]

Tc-99m-Pyrophosphate SPECT/CT

Clinically indicated Tc-99m-PYP SPECT/CT imaging was performed on a general-purpose cadmium-zinc-telluride-based imaging system (Veriton-CT; Spectrum Dynamics Inc) that was used to quantify radiotracer uptake as a surrogate marker for amyloid burden, as previously reported.[13] In brief, a single observer traced a volume of interest (VOI) along the 3-dimensional external LV contours of each patient on the CT scan, which was automatically mirrored to the fused SPECT

scan. An additional VOI in the center of the LA near the base was used to determine the blood pool activity; care was taken when drawing this VOI to minimize count spillover from the myocardium by drawing the VOI boundary with at least a pixel separation from the LA wall with PMOD Software (PMOD 4.3, PMOD Technologies LLC, Zurich, Switzerland). To correct for blood pool activity, an endocardial border of the LV VOI was drawn automatically by thresholding for 1.5× the mean standardized uptake value (g/mL) of the blood pool. The standardized uptake value was defined as the decay-corrected activity concentration of PYP divided by injected activity per unit body weight. The product of the VOI volume and mean standardized uptake value defined integrated cardiac amyloid activity.

Statistical Analysis

Statistical analysis was performed by IBM SPSS Statistics, version 28.0 (IBM Corporation, Armonk, NY) or GraphPad Prism 10.0.0 for Mac (GraphPad Software, Boston, MA). The test-retest repeatability was calculated by mean differences and standard deviations across all measurements for each participant; as data were not normally distributed, the median of mean differences and SD was given. Continuous variables are shown as median (IQR) for all data, normally and non-normally distributed. Comparison of continuous variables between groups was performed with Mann-Whitney *U* and Kruskal-Wallis tests. A Fisher exact test was used to compare differences between groups for binary variables. Spearman correlation analysis was used to determine correlation between iVP, echocardiographic, SPECT, and CMR metrics as well as serological biomarkers. Multivariate linear regression analysis was performed to predict iVP from other demographic and echocardiographic variables. Demographic variables included age and sex; our aim was to include 1 variable each for LV mass, LV systolic and diastolic function, as well as RV function. If multiple variables were available (eg, indexed left ventricular mass [LVMi] and wall thickness, ejection fraction [EF], and GLS), the metric with the highest correlation to iVP was included.

RESULTS

Study Population

The study cohort consisted of 54 participants, including 10 patients with HCM, 28 with CA, and 16 healthy volunteers. All HCM patients had typical asymmetrical septal hypertrophy, including 3 with a sarcomeric variant. Five HCM patients had LV outflow tract obstruction. Among these, 3 participants had LV outflow tract obstruction at rest (median LV outflow tract gradient, 93 mm Hg) and 2 participants with Valsalva only (median LV outflow tract gradient, 56 mm Hg). In HCM, median ECV was 32% (IQR, 29%–34%), with normal ECV in 3 of 5 participants (60%). In addition, 4 participants had evidence of systolic anterior motion of the anterior mitral leaflet, including 1 participant with moderate mitral regurgitation and 2 participants with mild to moderate mitral regurgitation. The other 7 HCM participants had trace or mild mitral regurgitation. Among patients with CA, 21 patients had ATTR amyloidosis (including 4 with variant ATTR CA). The baseline characteristics are listed in Table 1.

Table S1 outlines conventional echocardiographic metrics. Although septal thickness, cardiac volumes, and LA size did not differ between CA and HCM, systolic and diastolic LV function as well as LA and RV function were worse in CA.

Normal Limits and Repeatability of Myocardial Stiffness by Intrinsic Velocity Propagation

In healthy volunteers, median iVP was 1.4 m/s (IQR, 1.3–1.5 m/s; range, 0.9–1.8 m/s), with an upper limit of normal (95th percentile) at 1.7 m/s. Across 9 measurements in each participant, iVP was highly repeatable with a median of mean differences of 0 m/s (IQR, −0.1 to 0.1; range, −0.3 to 0.3) and a median of standard deviations of 0.3 m/s (IQR, 0.2–0.5; range, 0.1–0.7).

Intrinsic Velocity Propagation Estimated Myocardial Stiffness in HCM and Amyloidosis

In HCM, the median iVP was 1.4 m/s (IQR, 1.0–1.8 m/s; range, 0.8–1.9 m/s) with a median of mean differences of 0.1 m/s (IQR, −0.1 to 0.2; range, −1.0 to 0.3) and a median of standard deviations of 0.3 m/s (IQR, 0.1–0.7; range, 0.1–1.0).

In CA, the median iVP was 2.6 m/s (IQR, 1.7–3.9 m/s; range, 0.8–7.8 m/s) with a median of mean differences of 0 m/s (IQR, −0.5 to 0.4; range, −2.8 to 3.3) and a median of standard deviations of 1.1 m/s (IQR, 0.4–2.7; range, 0.1–8.3). iVP differed significantly across study groups ($P<0.001$; Figure 1). After Bonferroni correction for multiple tests, iVP remained higher in CA than in HCM ($P=0.011$) and healthy volunteers ($P=0.001$). However, it did not differ between HCM and healthy volunteers ($P=0.926$).

Univariable and Multivariable Associations of Intrinsic Velocity Propagation Estimated Myocardial Stiffness

As shown below, iVP correlates with cardiac structure, diastolic and systolic function, cardiac biomarkers, and amyloid burden in the pooled HCM and CA cohorts. Correlations between iVP and other variables are listed in Table S2 for the pooled and for the separate patient cohorts of HCM and CA, respectively. In CA, the magnitude of correlation was lower for age, LA strain, LV volumes, and biventricular EF (from CMR) but higher for E/e' than in HCM. For the rest of the results section, correlations include the pooled cohort of patients (ie, CA and HCM).

Diastolic Function

Markers of diastolic function correlated moderately with myocardial stiffness in HCM and CA: mean E/e' ($\rho=0.399$; Figure 2A), estimated systolic pulmonary artery pressure ($\rho=0.459$), LA contraction strain

Table 1. Clinical Characteristics

	Cardiac amyloidosis (n=28)					
	All (n=28)	ATTR (n=21)	AL (n=7)	*P* value	HCM (n=10)	*P* value (CA vs HCM)
Demographics						
Age, y	73 [67–80]	77 [69–81]	66 [45–73]	0.007	55 [32–66]	<0.001
Female, n (%)	5 (18)	2 (10)	3 (43)	0.046	2 (20)	0.881
Non-Hispanic White, n (%)	24 (86)	19 (91)	5 (71)	0.212	9 (90)	0.731
Signs and symptoms						
Dyspnea, n (%)	11 (36)	7 (33)	4 (57)	0.264	3 (30)	0.601
Lower leg edema, n (%)	10 (36)	5 (24)	5 (71)	0.023	0 (0)	0.028
Carpal tunnel syndrome, n (%)	18 (64)	17 (81)	1 (14)	0.001	0 (0)	<0.001
Biceps tendon rupture, n (%)	8 (29)	8 (38)	0 (0)	0.053	1 (10)	<0.001
Comorbidities						
Hypertension, n (%)	16 (57)	12 (57)	4 (57)	1.000	4 (40)	0.351
Diabetes, n (%)	2 (7)	2 (10)	0 (0)	0.397	2 (20)	0.255
Coronary artery disease, n (%)	5 (18)	4 (19)	1 (14)	0.738	2 (20)	0.919
Atrial fibrillation, n (%)	10 (36)	8 (38)	2 (29)	0.649	3 (30)	0.744
Medication						
Tafamidis, n (%)	19 (68)	19 (91)	0 (0)	<0.001	0 (0)	<0.001
Laboratory findings						
TTR mutation, n (%)	4 (14)	4 (19)	0 (0)	0.078	0 (0)	0.112
Sarcomeric mutation, n (%)	NA	NA	NA	NA	3 (30)	NA
eGFR, mL/min per 1.73 m^2	73 [57–81]	74 [58–84]	72 [48–77]	0.640	95 [91–100]	<0.001
NT-proBNP, ng/L	1506 [637–2868]	1513 [634–2762]	999 [449–11575]	0.935	459 [123–731]	0.019
Troponin T, ng/mL	35 [24–62]	34 [21–58]	40 [28–96]	0.387	8 [8–8]	0.148

Values given are median [interquartile range] or number (%). Comparison was performed by Mann-Whitney *U* test or Fisher exact test, respectively. AL indicates light chain; ATTR, transthyretin; CA, cardiac amyloidosis; HCM, hypertrophic cardiomyopathy; eGFR, estimated glomerular filtration rate; NT-proBNP, N-terminal pro-B-type natriuretic peptide; and TTR, transthyretin.

(ρ=0.515), and LA reservoir strain (ρ=−0.548; Figure 2B) correlated moderately with iVP. Indexed LA volume did not correlate with iVP (ρ=0.005).

Structure and Systolic Function in Echocardiography

Indexed LV mass correlated weakly with iVP (LVMi; ρ=0.379). Markers of systolic function correlated moderately with myocardial stiffness in HCM and CA: LV EF (ρ=−0.388), GLS (ρ=0.453; Figure 2C), RV fractional area change (ρ=−0.393), and RV free wall strain (ρ=0.491; Figure 2D) correlated moderately with iVP. Multivariate linear regression analysis, including age, sex, LVMi, GLS, RV free wall strain, and E/e', significantly predicted iVP (F(6,30)=3.9, *P*=0.005, R^2=0.440). RV free wall strain (*P*=0.033) and E/e' (*P*=0.029) contributed to the prediction, but age (*P*=0.795), sex (*P*=0.461), LVMi (*P*=0.620), and GLS (*P*=0.503) did not. Model coefficients and CIs are reported in Table S3.

Structure and Systolic Function in Cardiac Magnetic Resonance Imaging

In a subgroup of 22 patients (17 CA and 5 HCM) who underwent cardiac magnetic resonance imaging, there was a moderate correlation of iVP with LVMi (ρ=0.505; Figure 3A) and a strong correlation of iVP with indexed RV end-diastolic (ρ=0.731) and end-systolic volume (ρ=0.604) but no significant correlation with LVEF, indexed LV end-diastolic volume, indexed LV end-systolic volume, or RVEF (ρ<0.400, *P*>0.05).

Cardiac Biomarkers

iVP moderately correlated with NT-proBNP (N-terminal pro-B-type natriuretic peptide; ρ=0.498; Figure 3B) and troponin T (ρ=0.382).

Interstitial Expansion (ECV)

Among a subgroup of 22 patients, iVP correlated moderately with interstitial expansion as measured by ECV (ρ=0.646, *P*=0.004; Figure 3C).

Multiple linear regression analysis including iVP, LVMi (from CMR), GLS, and E/e' significantly predicted ECV (F(4,13)=3.7, *P*=0.048, R^2=0.621). iVP (*P*=0.018) contributed to the prediction, but LVMi (*P*=0.659), GLS (*P*=0.181), and E/e' (*P*=0.499) did not. Model coefficients and CIs are reported in Table S3.

Amyloid Burden

Among a subgroup of 10 patients (9 CA and 1 HCM) with PYP SPECT/CT, iVP correlated strongly with amyloid burden as measured by cardiac amyloid

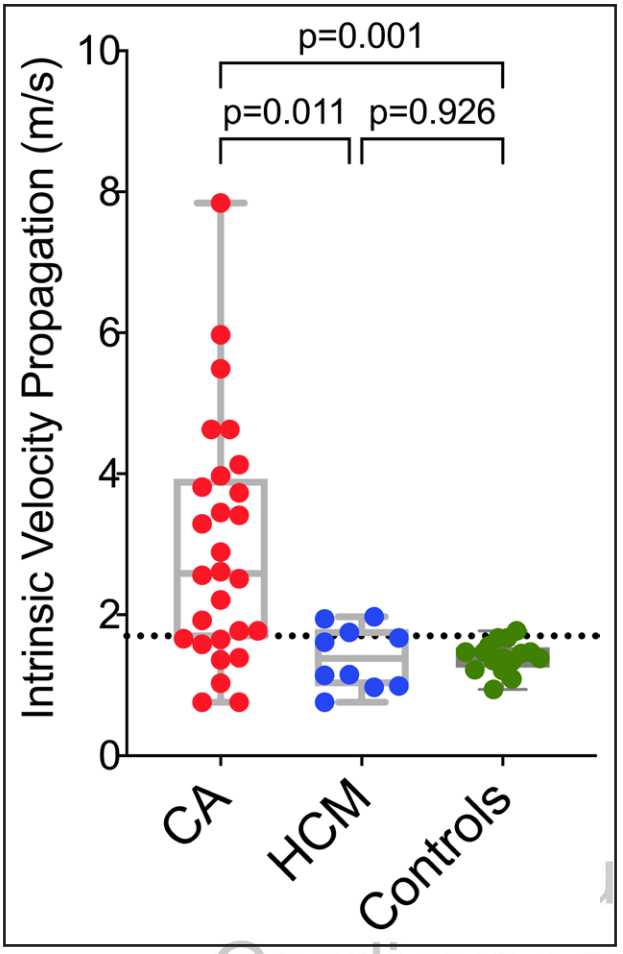

Figure 1. Myocardial stiffness across study groups. The scatter and box plot outlines intrinsic velocity propagation in cardiac amyloidosis (CA, n=28), hypertrophic cardiomyopathy (HCM, n=10), and healthy volunteers (controls, n=16). After Bonferroni correction for multiple tests, intrinsic velocity propagation is significantly higher in CA than in HCM or healthy volunteers. Comparison was performed by Kruskal-Wallis test. The dotted line indicates the upper limit of normal (95th percentile in healthy volunteers).

activity (ρ=0.891, *P*<0.001; Figure 3D). Multivariate linear regression analysis including iVP, GLS, and E/e' trended to predict cardiac amyloid activity (F(3,5)=4.5, *P*=0.069, R^2=0.731). iVP (*P*=0.031) contributed to the prediction, but GLS (*P*=0.175) and E/e' (*P*=0.522) did not. Model coefficients and CIs are reported in Table S3.

Clinical Correlates of Normal Myocardial Stiffness in CA

Among participants with CA (n=28), 8 participants (29%) had normal myocardial stiffness (<1.7 m/s), including 2 participants with AL amyloidosis (Table 2). Amyloidosis participants with normal myocardial stiffness were characterized by lower NT-proBNP (*P*=0.034), troponin T (*P*=0.041), National Amyloidosis Center stage (*P*=0.031), and interstitial expansion (median ECV, 33% versus 53%; *P*=0.077)/amyloid burden (median cardiac amyloid activity, 125 versus 874; *P*=0.056). All other clinical and echocardiographic metrics (except for deceleration time) did not differ between CA patients with normal versus increased myocardial stiffness (Table 2).

DISCUSSION

Intrinsic cardiac elastography is emerging as a noninvasive tool to measure myocardial stiffness in various forms of myocardial diseases.[1,14] This study demonstrates and confirms that myocardial stiffness can be measured by echocardiography with high repeatability and correlates with cardiac structure and function but is mainly related to myocardial tissue abnormalities such as interstitial remodeling and amyloid burden. Our findings also highlight that low myocardial stiffness may differentiate early from advanced disease and serve as a marker for low amyloid burden in CA (Figure 4). Considering that cardiac structure, function, hemodynamics, and myocardial stiffness all affect clinical manifestations of heart failure, intrinsic cardiac elastography may complement and advance the existing echocardiographic assessment of CA.

Feasibility of the Method

In its present version, intrinsic cardiac elastography is feasible with high repeatability in participants with an atrial contraction, requiring a single additional image loop (apical 4-chamber view focused on septum) and several steps of postprocessing but without the need for refined hardware. While the present study tested a research prototype, updated versions of the software could be installed on commercially available devices. Comparable approaches for intrinsic cardiac elastography from other vendors are commercially available using state-of-the-art clinical equipment.[15]

At frame rates above 250 m/s, this study focused on mechanical waves induced by atrial contraction/kick, which propagated at speeds around 1 and 4 m/s. For these mechanical waves, undetected atrial fibrillation or RV pacing were the main reasons for method failure. While shear waves from valve closure would have been affected less by arrhythmias, they overall have lower proportions of accepted waves (52% versus 86%) than pressure waves from atrial contraction, even at higher frame rates (ie, 800–1400 fps).[3] In accordance with previous publications, the feasibility for mechanical waves from atrial contraction in the present study is high.[1,3,16] Similarly, the variation of mechanical wave speeds from atrial contraction compares well to prior studies in healthy volunteers (ie, 82% of measurements had an SD of <0.3 m/s)[16] and underscores the reliability of the method overall. However, we investigated the repeatability in all groups separately and identified a higher variation in

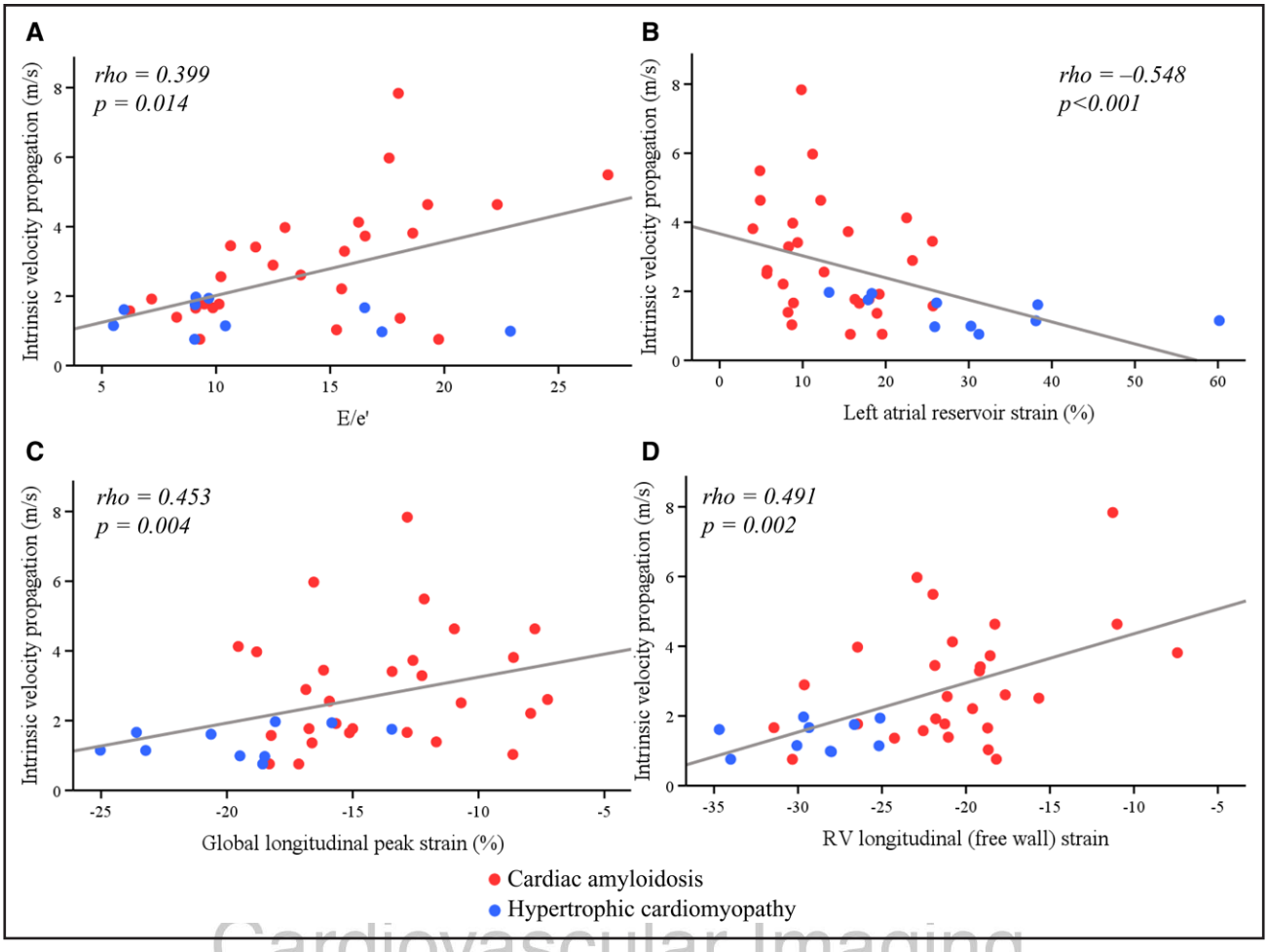

Figure 2. Relationship of myocardial stiffness with systolic and diastolic function.
The scatter plots display the correlations between intrinsic velocity propagation and E/e' (**A**), left atrial reservoir strain (**B**), global longitudinal peak strain (**C**), and right ventricular (RV) longitudinal free wall strain (**D**).

CA than in healthy volunteers (ie, median of SDs, 1.1 versus 0.3 m/s). Although this could reflect hemodynamic or pathobiological alterations to some degree, it demarcates the boundaries of this method at the most advanced myocardial stiffness. Further technological refinements are therefore needed to enhance the temporal resolution and smoothen the isovelocity wave front when propagation speeds become high.

Myocardial Stiffness in Cardiac Diseases

Normal values of mechanical wave speeds depend on the applied technique (intrinsic versus extrinsic), localization (septum versus lateral wall), and inducing event (atrial contraction versus valve closure).[3,17,18] For intrinsic cardiac elastography of the atrial contraction throughout the inferoseptal wall, mechanical wave speeds around 1.3 and 1.4 m/s have been reported[1,3] and consolidate our measurements in healthy volunteers (ie, 1.4 m/s).

In our cohort of patients with CA, 25% of participants had mechanical wave speeds <1.7 m/s falling into values similar to healthy volunteers. These participants had lower NT-proBNP and troponin as well as lower cardiac amyloid burden (by CMR and SPECT). This reflects prior data in pigs where changes in loading conditions and in myocardial tissue properties were the main factors to influence myocardial stiffness (invasively and in intrinsic cardiac elastography).[1,19] Furthermore, it also explains the inability of intrinsic cardiac elastography to differentiate CA from HCM at mechanical wave speeds below 2 m/s. At earlier stages of the disease and normal loading conditions, myocardial stiffness might not yet be affected. Accordingly, lower mechanical wave speeds were associated with better outcomes in a prior publication,[5] highlighting the prognostic value of noninvasive measurement of myocardial stiffness.

Our HCM cohort had normal systolic and diastolic function, especially normal (or low) LV filling pressures indicated by a mean E/e' of 9 and an NT-proBNP of 459 ng/L. Furthermore, ECV was normal in the majority of HCM participants undergoing CMR. Therefore, mechanical wave speeds were substantially lower in the

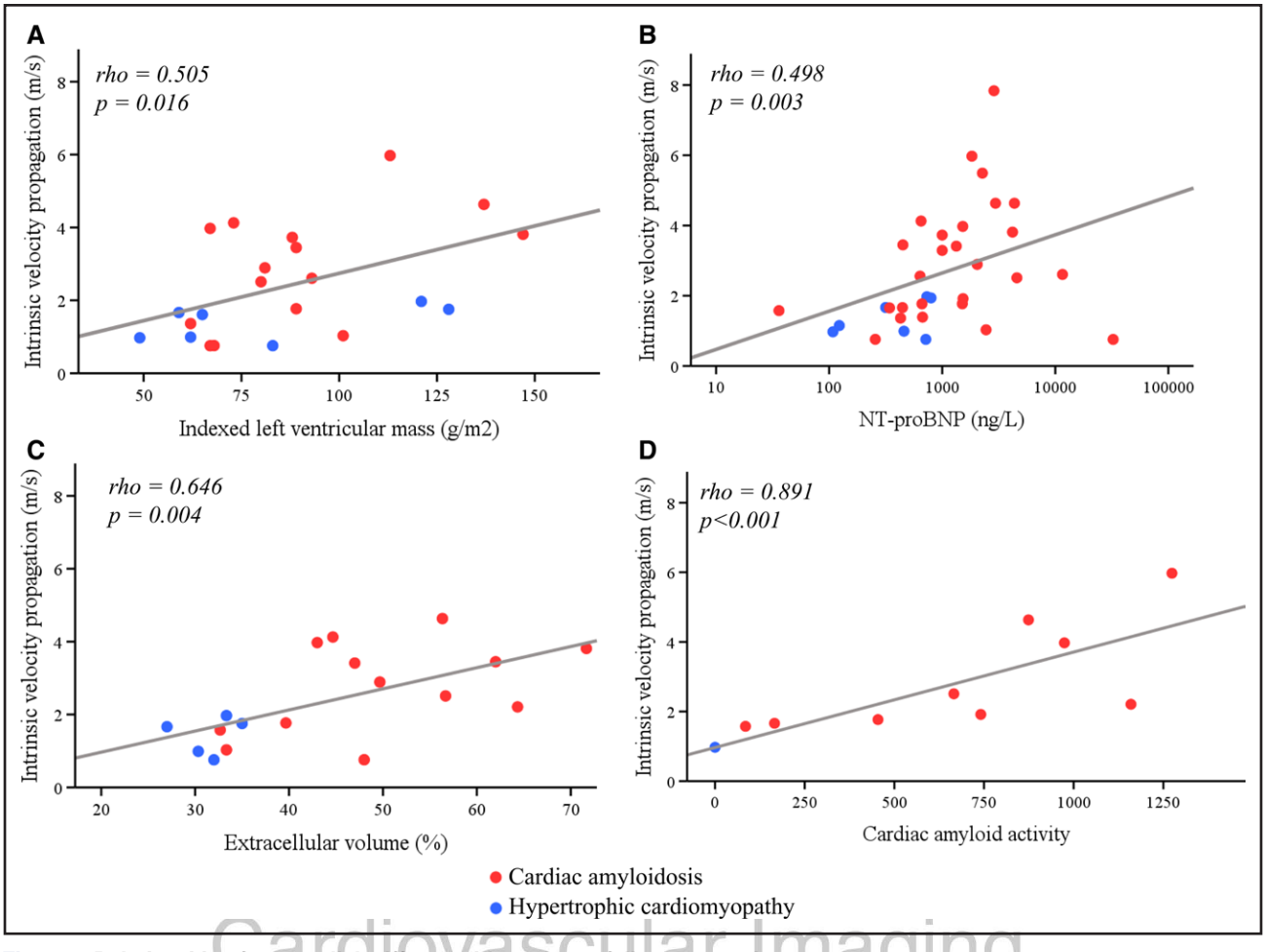

Figure 3. Relationship of myocardial stiffness with markers of disease severity.
The scatter plots display the correlations between intrinsic velocity propagation and indexed left ventricular mass from cardiac magnetic resonance imaging (**A**), NT-proBNP (N-terminal pro-B-type natriuretic peptide; **B**), extracellular volume (**C**), and cardiac amyloid activity from 99m-technetium-pyrophosphate single-photon emission computed tomography/computed tomography (**D**).

present study (ie, 1.4 m/s) compared with a prior study (ie, 2.9 m/s).[20] This difference may be explained by less advanced HCM in the present study. In particular, considering the close relationship between echocardiographic myocardial stiffness and histological quantification of interstitial fibrosis in the latter study,[20] the low ECV could serve as an explanation for the low myocardial stiffness in our HCM cohort. Conversely, the differences in myocardial stiffness between HCM and CA despite similar wall thickness (and the lack of difference between HCM and healthy volunteers despite differences in wall thickness) emphasize that myocardial stiffness is influenced by the underlying pathobiology and myocardial tissue abnormalities rather than increases in septal wall thickness.

Currently, ECV is the primary metric to quantify interstitial expansion from amyloid fibrils and fibrosis,[21] which has clinical implications for diagnosing, risk-stratifying, and monitoring the disease.[22–24] Interestingly, interstitial expansion by ECV is closely linked to specific functional and structural abnormalities; for example, while at low ECV the LV mass, strain, or E/e' are abnormal in most patients, LVEF or LA size only become abnormal at high ECV.[25] While ECV images structural abnormalities, intrinsic cardiac elastography provides a signal of function. This study expands the relationship between amyloid burden and functional alterations to myocardial stiffness. Indeed, myocardial stiffness is much more prominent in CA than in HCM (despite similar LV wall thickness) but also in CA with high versus low disease burden.

Clinical Implications

Intrinsic cardiac elastography meets an unmet need of clinical cardiology to quantify myocardial stiffness and estimate the extent of myocardial tissue abnormalities in daily practice by echocardiography. This noninvasive, easily accessible, and highly reproducible approach advances the field in multiple directions. First, the assessment of myocardial stiffness by intrinsic cardiac elastography emerges as an alternative (or complementary) avenue to the complex multiparametric approach to classify and stage diastolic dysfunction.[26] Improved disease staging

Table 2. Characteristics of Normal Myocardial Stiffness in Cardiac Amyloidosis

	Normal myocardial stiffness (n=8)	Increased myocardial stiffness* (n=20)	*P* value
Demographics			
Age, y	73 [65 to 78]	73 [67 to 80]	0.823
Female, n (%)	2 (25)	3 (15)	0.533
Non-Hispanic White, n (%)	8 (100)	16 (80)	0.172
NAC stage I, n (%)	7 (87)	13 (65)	0.031
Signs and symptoms			
Dyspnea, n (%)	1 (13)	10 (50)	0.066
Lower leg edema, n (%)	1 (13)	9 (45)	0.105
Carpal tunnel syndrome, n (%)	5 (63)	13 (65)	0.901
Biceps tendon rupture, n (%)	3 (38)	5 (25)	0.508
Comorbidities			
Hypertension, n (%)	4 (50)	12 (60)	0.629
Diabetes, n (%)	0 (0)	2 (10)	0.353
Coronary artery disease, n (%)	1 (13)	4 (20)	0.601
Atrial fibrillation, n (%)	3 (38)	7 (35)	0.901
AL amyloidosis, n (%)	2 (25)	5 (25)	1.000
Medication			
Tafamidis, n (%)	5 (63)	14 (70)	0.701
Laboratory findings			
TTR gene variant, n (%)	2 (25)	2 (10)	0.203
eGFR, mL/min per 1.73 m^2	65 [47 to 80]	75 [59 to 84]	0.237
NT-proBNP, ng/L	437 [278 to 1999]	1528 [999 to 2960]	0.034
Troponin T, ng/mL	25 [11 to 32]	46 [25 to 72]	0.041
LV structure			
Septal thickness, mm	18 [13 to 24]	20 [18 to 23]	0.304
EDD, mm	43 [39 to 44]	41 [38 to 47]	0.746
ESD, mm	31 [25 to 33]	31 [28 to 34]	0.784
Indexed mass, g/m^2	132 [107 to 173]	174 [133 to 214]	0.055
EDVi, mL/m^2	62 [54 to 66]	50 [40 to 64]	0.199
ESVi, mL/m^2	27 [24 to 30]	23 [20 to 34]	0.566
LV systolic function			
LVEF, %	57 [53 to 59]	53 [43 to 59]	0.281
GLS, %	−15.9 [−18.0 to −12.0]	−13.1 [−16.5 to −10.8]	0.281
RELAPS ratio	0.93 [0.88 to 1.07]	1.07 [0.96 to 1.61]	0.063
LV diastolic function			
E/A	1.2 [1.1 to 2.2]	2.5 [1.5 to 3.5]	0.073
Deceleration time, ms	226 [206 to 286]	162 [140 to 203]	0.007
Lateral e', cm/s	8 [5 to 10]	6 [5 to 7]	0.217
Septal e', m/s	6 [4 to 7]	5 [4 to 7]	0.658
Mean E/e'	10 [8 to 17]	15 [11 to 18]	0.119
sPAP, mm Hg	32 [23 to 37]	38 [30 to 42]	0.142
LA structure and function			
LA diameter, mm	44 [41 to 50]	48 [40 to 54]	0.328
LAVi, mL/m^2	50 [40 to 62]	47 [39 to 57]	0.862
Conduit strain, %	−9.7 [−14.8 to −5.1]	−7.1 [−11.6 to −5.1]	0.709
Contraction strain, %	−5.0 [−8.7 to −3.7]	−3.5 [−6.4 to −1.3]	0.182
Reservoir strain, %	16.3 [8.7 to 19.4]	10.5 [6.2 to 17.6]	0.258
RV structure and function			
Indexed RV area, cm^2/m^2	10.0 [9.0 to 11.2]	11.0 [8.8 to 12.8]	0.469
FAC, %	44 [40 to 53]	41 [34 to 50]	0.258
TAPSE, mm	16 [15 to 19]	16 [10 to 20]	0.500
S', cm/s	12.8 [9.0 to 13.6]	11.4 [9.2 to 14.5]	0.766
4-chamber strain, %	−17.7 [−21.9 to −14.2]	−16.3 [−18.7 to −12.6]	0.218
Free wall strain, %	−21.8 [−28.8 to −18.7]	−20.2 [−21.9 to −17.8]	0.258

Values given are median [interquartile range] or number (%). Comparison was performed by Mann-Whitney *U* test or Fisher exact test, respectively. AL indicates light chain; EDD, end-diastolic diameter; EDVi, indexed end-diastolic volume; eGFR, estimated glomerular filtration rate; ESD, end-systolic diameter; ESVi, indexed end-systolic volume; FAC, fractional area change; GLS, global longitudinal strain; LA, left atrial; LAVi, indexed left atrial volume; LV, left ventricular; LVEF, left ventricular ejection fraction; NAC, national amyloidosis center; NT-proBNP, N-terminal pro-B-type natriuretic peptide; RELAPS, relative apical sparing; RV, right ventricular; sPAP, estimated systolic pulmonary artery pressure; TAPSE, tricuspid annular plane systolic excursion; and TTR, transthyretin.

*Based on the 95th percentile in controls (ie, intrinsic velocity propagation ≥1.7 m/s).

may better identify patients with a more favorable treatment response. However, the method should not serve as a diagnostic tool to differentiate between cardiomyopathies. Second, and probably even more relevant, intrinsic cardiac elastography may provide novel information to unveil an echocardiographic window into disease biology. Finally, intrinsic elastography, in the future, could provide us a novel metric to evaluate a functional change following disease-modifying therapy.

Myocardial stiffness is a critical factor for the development of heart failure in any degree of myocardial disease. It provides the missing link between molecular tissue alterations and signs and symptoms of heart failure and may assist clinicians to better characterize these patients and their myocardium. Considering that LV filling pressures and myocardial tissue abnormalities both influence myocardial stiffness,[19] intrinsic cardiac elastography may guide management of fluid status over time and inform about diuretic dosing. After successful unloading,

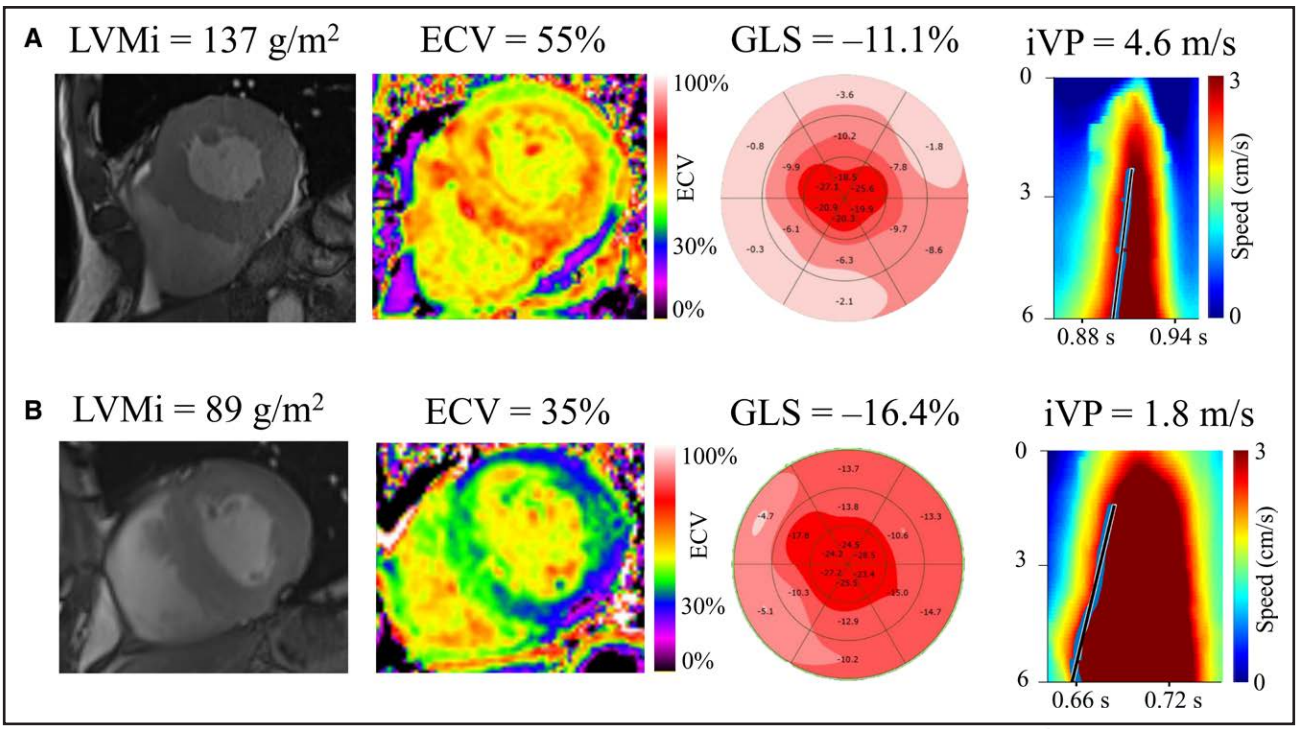

Figure 4. Case examples.
A, Illustrates an 84-year-old male at an advanced stage (National Amyloidosis Center [NAC] stage 3) of cardiac ATTR (transthyretin) amyloidosis testing. In echocardiography, indexed left ventricular mass (LVMi; 137 g/m^2), wall thickness (24 mm), E/e' (22), and indexed left atrial volume (57 mL/m^2) were increased, and his global longitudinal strain (GLS, −11.1%) was severely reduced. Extracellular volume (ECV, 55%) and cardiac amyloid activity (925) as markers of amyloid burden confirmed advanced cardiac disease. In line with these findings, intrinsic velocity propagation (iVP) was fast at 4.6 m/s, suggesting high myocardial stiffness. **B**, Displays a 72-year-old male at an early stage of cardiac ATTR amyloidosis (NAC stage 1). In echocardiography, indexed left ventricular mass (89 g/m^2) and E/e' (10) were normal, while wall thickness (15 mm) and indexed left atrial volume (67 mL/m^2) were increased. The GLS (−11.1%) was mildly reduced. ECV (35%) and cardiac amyloid activity (636) confirmed early cardiac disease. Accordingly, iVP was slow at 1.8 m/s, suggesting almost normal myocardial stiffness.

increased myocardial stiffness is more likely to indicate tissue alterations.

Limitations

The sample size, particularly for the comparison with CMR and SPECT, was relatively small. Nevertheless, the strong statistically significant associations support large effect sizes. The relatively small sample size, however, precludes subgroup analysis in AL and ATTR amyloidosis. The reference standard for myocardial stiffness is measured invasively on pressure volume loops. However, this information is not available in our cohort. Myocardial stiffness is load-dependent, and our study did not measure filling pressures of the heart invasively. Therefore, the study will not be able to distinguish increased myocardial stiffness from high LV filling measures and myocardial tissue abnormalities. However, we included outpatients on a stable diuretic regimen, limiting variability from loading conditions. It is probable that the amyloidosis cohort had a more advanced disease phenotype compared with the HCM cohort included in this study. Limited clinical information is available on the control cohort. The threshold for normal myocardial stiffness has been defined in the context of this study to assess clinical and imaging characteristics of a population with ATTR amyloidosis and normal myocardial stiffness; the threshold cannot be generalized and implemented on an individual level. In addition, our findings on echocardiographic myocardial stiffness are limited to the inferoseptal wall of the left ventricle. However, for a diffuse disease like amyloidosis, measures in the inferoseptum should be comparable to those of the other walls. In our experience and based on prior publications, feasibility to acquire valid measurements is highest at this location with the least confounding of the signal by cardiac motion, reverberation, and angle error.[3] The median frame rate in this study limits the temporal resolution and exact measurement of myocardial mechanical waves traveling at speeds of up to 4 m/s. However, a similar approach at comparable frame rates has previously demonstrated valid and robust measurements with clinical and prognostic value.[1,5,15]

Conclusions

Intrinsic cardiac elastography is a reliable noninvasive tool to measure myocardial stiffness. In this pilot study, it has high repeatability, is closely related to markers of

cardiac structure and function, interstitial remodeling and amyloid burden, and differentiates early from advanced disease stages in CA. Larger studies are warranted to define its value in myocardial tissue characterization and heart failure management.

ARTICLE INFORMATION

Received August 16, 2024; accepted December 20, 2024.

Affiliations

Cardiovascular Imaging and Amyloidosis Programs (D.C.B., O.F.C., J.C.N., A.T., S.V., S.A.M.C., R.H.F., S.D.) and Cardiovascular Division (C.Y.H.), Brigham and Women's Hospital, Harvard Medical School, Boston, MA. Philips Research, Cambridge, MA (A.S., P.R.).

Acknowledgments

The authors are extremely grateful to each of the study participants for making this study possible.

Sources of Funding

This study was supported by a research grant from Philips. Dr Benz was funded by Swiss National Science Foundation (grant number P400PM_199305) and a career development grant from the Advanced Clinician Scientist Program of University Medicine Zurich. Dr Clerc was supported by research fellowship from the International Society of Amyloidosis and Pfizer. Dr Dorbala was funded by NIH K24HL157648.

Disclosures

Dr Benz received investigator-initiated research funding from Astra Zeneca; consulting fees from Pfizer and Astra Zeneca; and travel support from Philips. Dr Cuddy received investigator-initiated research grant from Pfizer; and consulting fees from Ionis Pharmaceuticals, Astra Zeneca, BridgeBio, Novo Nordisk, and Pfizer. Dr Dorbala received consulting fees from Pfizer, GE Healthcare, Novo Nordisk, and Astra Zeneca; and investigator-initiated grants from Pfizer, Attralus, GE Healthcare, Phillips, and Siemens. Dr Falk received consulting fees from Ionis Pharmaceuticals, Alnylam Pharmaceuticals, and Caelum Biosciences; and research funding from GlaxoSmithKline and Akcea. Dr Ho received investigator-initiated research funding from Bristol Myers Squibb, Cytokinetics, Tenaya, and Biomarin; and consulting fees from Bristol Myers Squibb, Cytokinetics, Tenaya, Biomarin, viz.ai, Lexicon. Dr Sadeghi and P. Rafter are employed by Philips Research. The other authors report no conflicts.

Supplemental Material

Tables S1–S3
Figure S1

REFERENCES

1. Pislaru C, Pellikka PA, Pislaru SV. Wave propagation of myocardial stretch: correlation with myocardial stiffness. *Basic Res Cardiol*. 2014;109:438. doi: 10.1007/s00395-014-0438-5
2. Couade M, Pernot M, Messas E, Bel A, Ba M, Hagege A, Fink M, Tanter M. In vivo quantitative mapping of myocardial stiffening and transmural anisotropy during the cardiac cycle. *IEEE Trans Med Imaging*. 2011;30:295–305. doi: 10.1109/TMI.2010.2076829
3. Espeland T, Wigen MS, Dalen H, Berg EAR, Hammer TA, Salles S, Lovstakken L, Amundsen BH, Aakhus S. Mechanical wave velocities in left ventricular walls in healthy subjects and patients with aortic stenosis. *JACC Cardiovasc Imaging*. 2024;17:111–124. doi: 10.1016/j.jcmg.2023.07.009
4. Pislaru C, Alashry MM, Thaden JJ, Pellikka PA, Enriquez-Sarano M, Pislaru SV. Intrinsic wave propagation of myocardial stretch, a new tool to evaluate myocardial stiffness: a pilot study in patients with aortic stenosis and mitral regurgitation. *J Am Soc Echocardiogr*. 2017;30:1070–1080. doi: 10.1016/j.echo.2017.06.023
5. Pislaru C, Ionescu F, Alashry M, Petrescu I, Pellikka PA, Grogan M, Dispenzieri A, Pislaru SV. Myocardial stiffness by intrinsic cardiac elastography in patients with amyloidosis: comparison with chamber stiffness and global longitudinal strain. *J Am Soc Echocardiogr*. 2019;32:958–968.e4. doi: 10.1016/j.echo.2019.04.418
6. Dorbala S, Ando Y, Bokhari S, Dispenzieri A, Falk RH, Ferrari VA, Fontana M, Gheysens O, Gillmore JD, Glaudemans AWJM, et al. ASNC/AHA/ASE/EANM/HFSA/ISA/SCMR/SNMMI expert consensus recommendations for multimodality imaging in cardiac amyloidosis: part 2 of 2-diagnostic criteria and appropriate utilization. *Circ Cardiovasc Imaging*. 2021;14:e000030. doi: 10.1161/HCI.0000000000000030
7. Lang RM, Badano LP, Mor-Avi V, Afilalo J, Armstrong A, Ernande L, Flachskampf FA, Foster E, Goldstein SA, Kuznetsova T, et al. Recommendations for cardiac chamber quantification by echocardiography in adults: an update from the American Society of Echocardiography and the European Association of Cardiovascular Imaging. *J Am Soc Echocardiogr*. 2015;28:1–39.e14. doi: 10.1016/j.echo.2014.10.003
8. Thirion JP. Image matching as a diffusion process: an analogy with Maxwell's demons. *Med Image Anal*. 1998;2:243–260. doi: 10.1016/s1361-8415(98)80022-4
9. Salles S, Lovstakken L, Aase SA, Bjastad TG, Torp H. Clutter filter wave imaging. *IEEE Trans Ultrason Ferroelectr Freq Control*. 2019;66:1444–1452. doi: 10.1109/TUFFC.2019.2923710
10. Sadeghi A, Vignon F, Carrascal C, Rafter P. Myocardial stretch propagation measurement with focused and diverging beams: a feasibility and reproducibility study in healthy volunteers. 2020 IEEE International Ultrasonics Symposium (IUS). 2020:1–4. doi: 10.1109/IUS46767.2020.9251722
11. Fischler M, Bolles R. Random sample consensus: a paradigm for model fitting with applications to image analysis and automated cartography. *Commun ACM*. 1981;24:381–395. doi: 10.1145/358669.358692
12. Cuddy SAM, Bravo PE, Falk RH, El-Sady S, Kijewski MF, Park MA, Ruberg FL, Sanchorawala V, Landau H, Yee AJ, et al. Improved quantification of cardiac amyloid burden in systemic light chain amyloidosis: redefining early disease? *JACC Cardiovasc Imaging*. 2020;13:1325–1336. doi: 10.1016/j.jcmg.2020.02.025
13. Dorbala S, Park MA, Cuddy S, Singh V, Sullivan K, Kim S, Falk RH, Taqueti VR, Skali H, Blankstein R, et al. Absolute quantitation of cardiac 99mTc-pyrophosphate using cadmium-zinc-telluride-based SPECT/CT. *J Nucl Med*. 2021;62:716–722. doi: 10.2967/jnumed.120.247312
14. Caenen A, Bézy S, Pernot M, Nightingale KR, Vos HJ, Voigt JU, Segers P, D'hooge J. Ultrasound shear wave elastography in cardiology. *JACC Cardiovasc Imaging*. 2024;17:314–329. doi: 10.1016/j.jcmg.2023.12.007
15. Pislaru C, Alashry MM, Ionescu F, Petrescu I, Pellikka PA, Grogan M, Dispenzieri A, Pislaru SV. Increased myocardial stiffness detected by intrinsic cardiac elastography in patients with amyloidosis: impact on outcomes. *JACC Cardiovasc Imaging*. 2019;12:375–377. doi: 10.1016/j.jcmg.2018.08.014
16. Kvåle KF, Salles S, Lervik LCN, Støylen A, Løvstakken L, Samset E, Torp H. Detection of tissue fibrosis using natural mechanical wave velocity estimation: feasibility study. *Ultrasound Med Biol*. 2020;46:2481–2492. doi: 10.1016/j.ultrasmedbio.2020.04.022
17. Villemain O, Correia M, Mousseaux E, Baranger J, Zarka S, Podetti I, Soulat G, Damy T, Hagège A, Tanter M, et al. Myocardial stiffness evaluation using noninvasive shear wave imaging in healthy and hypertrophic cardiomyopathic adults. *JACC Cardiovasc Imaging*. 2019;12:1135–1145. doi: 10.1016/j.jcmg.2018.02.002
18. Petrescu A, Santos P, Orlowska M, Pedrosa J, Bézy S, Chakraborty B, Cvijic M, Dobrovie M, Delforge M, D'hooge J, et al. Velocities of naturally occurring myocardial shear waves increase with age and in cardiac amyloidosis. *JACC Cardiovasc Imaging*. 2019;12:2389–2398. doi: 10.1016/j.jcmg.2018.11.029
19. Bézy S, Duchenne J, Orlowska M, Caenen A, Amoni M, Ingelaere S, Wouters L, McCutcheon K, Minten L, Puvrez A, et al. Impact of loading and myocardial mechanical properties on natural shear waves: comparison to pressure-volume loops. *JACC Cardiovasc Imaging*. 2022;15:2023–2034. doi: 10.1016/j.jcmg.2022.07.011
20. Naser JA, Anupraiwan O, Adigun RO, Maleszewski JJ, Pislaru SV, Pellikka PA, Pislaru C. Myocardial stiffness by cardiac elastography in hypertrophic cardiomyopathy: relationship with myocardial fibrosis and clinical outcomes. *JACC Cardiovasc Imaging*. 2021;14:2051–2053. doi: 10.1016/j.jcmg.2021.05.024
21. Pucci A, Aimo A, Musetti V, Barison A, Vergaro G, Genovesi D, Giorgetti A, Masotti S, Arzilli C, Prontera C, et al. Amyloid deposits and fibrosis on left ventricular endomyocardial biopsy correlate with extracellular volume in cardiac amyloidosis. *J Am Heart Assoc*. 2021;10:e020358. doi: 10.1161/JAHA.120.020358
22. Mongeon FP, Jerosch-Herold M, Coelho-Filho OR, Blankstein R, Falk RH, Kwong RY. Quantification of extracellular matrix expansion by CMR in infiltrative heart disease. *JACC Cardiovasc Imaging*. 2012;5:897–907. doi: 10.1016/j.jcmg.2012.04.006
23. Fontana M, Pica S, Reant P, Abdel-Gadir A, Treibel TA, Banypersad SM, Maestrini V, Barcella W, Rosmini S, Bulluck H, et al.

Prognostic value of late gadolinium enhancement cardiovascular magnetic resonance in cardiac amyloidosis. *Circulation*. 2015;132:1570–1579. doi: 10.1161/CIRCULATIONAHA.115.016567

24. Rettl R, Mann C, Duca F, Dachs TM, Binder C, Ligios LC, Schrutka L, Dalos D, Koschutnik M, Donà C, et al. Tafamidis treatment delays structural and functional changes of the left ventricle in patients with transthyretin amyloid cardiomyopathy. *Eur Heart J Cardiovasc Imaging*. 2022;23:767–780. doi: 10.1093/ehjci/jeab226
25. Knight DS, Zumbo G, Barcella W, Steeden JA, Muthurangu V, Martinez-Naharro A, Treibel TA, Abdel-Gadir A, Bulluck H, Kotecha T, et al. Cardiac structural and functional consequences of amyloid deposition by cardiac magnetic resonance and echocardiography and their prognostic roles. *JACC Cardiovasc Imaging*. 2019;12:823–833. doi: 10.1016/j.jcmg.2018.02.016
26. Smiseth OA, Morris DA, Cardim N, Cikes M, Delgado V, Donal E, Flachskampf FA, Galderisi M, Gerber BL, Gimelli A, et al; Reviewers: This document was reviewed by members of the 2018–2020 EACVI Scientific Documents Committee. Multimodality imaging in patients with heart failure and preserved ejection fraction: an expert consensus document of the European Association of Cardiovascular Imaging. *Eur Heart J Cardiovasc Imaging*. 2022;23:e34–e61. doi: 10.1093/ehjci/jeab154